Supporting Information

Bekinschtein *et al.* 10.1073/pnas.0809667106

SI Text

Local Field Potentials Recording and Processing. Two patients suffering from drug-refractory epilepsy were stereotactically implanted as part of a presurgical evaluation with depth electrodes (Ad-Tech Medical Instruments). Electrodes were 2.3 mm long with 1-mm diameter cylinders and an interelectrodes distance of 10 mm. The local field potential was digitized at 400 Hz from intracerebral electrodes referenced to the vertex (Nicolet). Epochs were then extracted (−200 ms plus 1,300 ms from first sound onset). Electrodes with a rejection rate >35% in relation to ample slow wave of epileptic figures were discarded. Remaining electrodes were submitted to automatic artifact rejection (+-300 μV threshold), visually inspected, low-pass-filtered (70 Hz), and notch-filtered (50 Hz) by using EEGLAB software (39). Baseline correction before fifth sound onset was applied and potentials were then averaged.

Experimental conditions were compared by using sample-by-sample *t* tests, with a first criterion of $P < 0.05$ for a minimum of 10 consecutive samples. Once an effect satisfied this first criterion, we counted the observed number of consecutive samples ($> = 10$) satisfying this criterion, and we also checked if the observed effect resisted to more conservative thresholds (10 consecutive samples at $P < 0.01$, 0.005, 0.001, 0.0005, and 0.0001). We kept the more conservative observed criteria (e.g., 10 samples at $P < 0.001$ or 35 samples at $P < 0.05$), and further checked the statistical significance of this observed effect through Monte Carlo permutations following we described elsewhere (40, 41). This procedure is particularly relevant to estimate the statistical significance of effects observed with a signal of unknown distribution (42). For each patient and for each electrode showing a significant effect, we computed 1,000 random permutations of the observed trials in 2 surrogate conditions; for each permutation, we then counted the number of surrogate effects satisfying our criterion. We then computed the observed probability of this criterion (number of surrogate effects per 1,000) and used this proportion as an estimate of the first-order α risk. For each patient and each electrode, this P value was <0.05.

fMRI. We used a 3-Tesla body system (Siemens) and a gradient echoplanar-imaging sequence sensitive to brain oxygen-level-dependent (BOLD) signal (44 contiguous axial slices, 3 mm thickness; TR = 2400 ms; angle = 90°, TE = 30 ms, in-plane resolution = $3 \times 3 \times 3$ mm3, matrix = $64 \times 64 \times 44$). In each run, 100 functional volumes were acquired. The first 2 volumes were discarded to reach equilibrium. T1-weighted images were also acquired for anatomical localization. Data processing, performed with SPM5 software, included corrections for EPI distortion, slice acquisition time, and motion; normalization; Gaussian smoothing (5-mm FWHM); fitting with a linear combination of functions derived by convolving a standard hemodynamic response with the time series of the 4 stimulus types, time-locked with the onset of the fifth sound of stimuli (local standard/deviant × global standard/deviant). We then ran a second-level random-effect group analysis, with a voxelwise threshold $P < 0.01$ and cluster size threshold of $P < 0.05$ corrected for multiple comparisons across the whole brain. We contrasted local deviant minus local standard trials, and global deviant minus global standard trials (see Table S1).

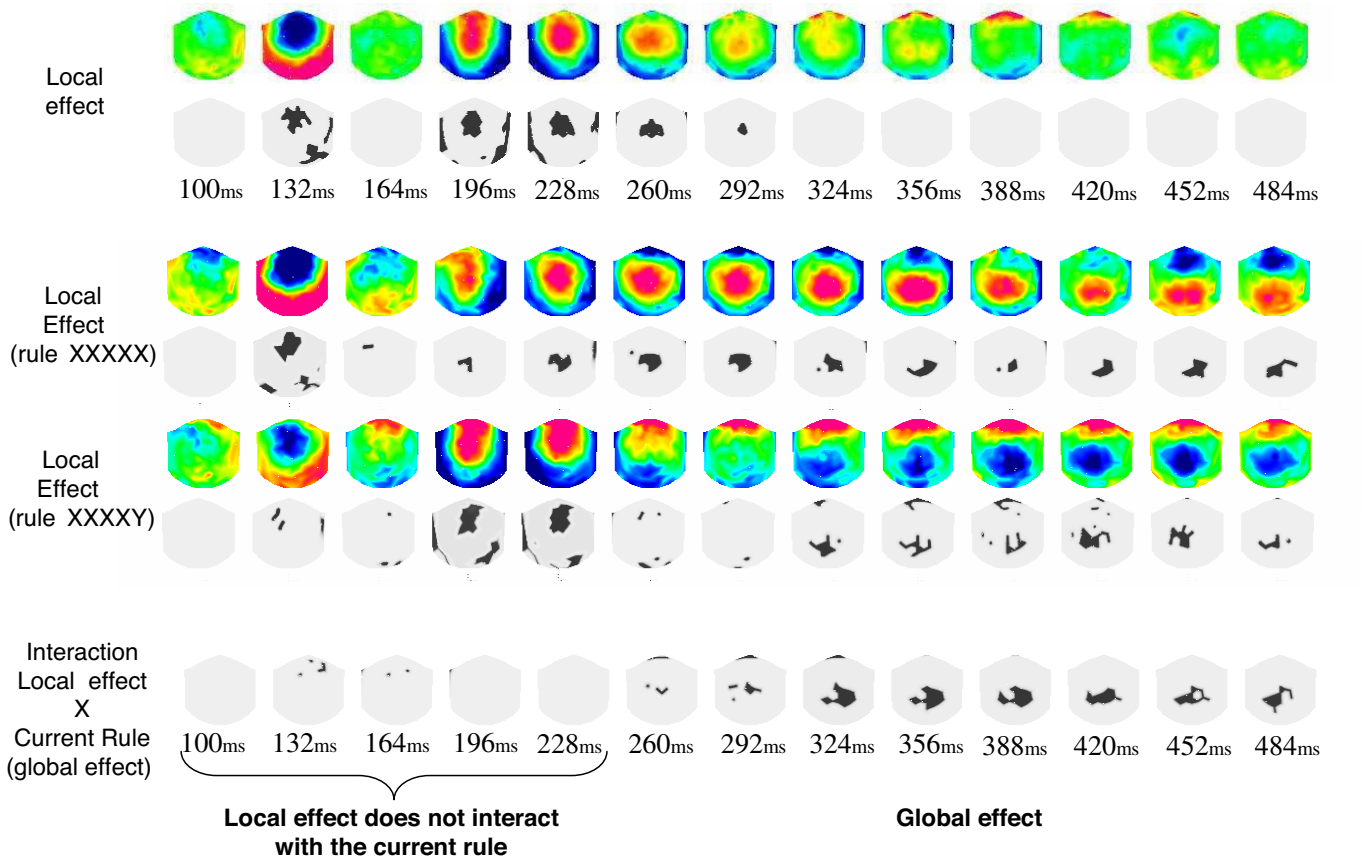

Fig. S1. Local effect split by current global regularity in the counting group. Averaged voltage scalpmaps of the local effect subtractions are plotted separately for the two global rules (LDGD-LSGS and LDGS-LSGD) (top) from 100 to 484 ms after the onset of the fifth sound. Corresponding thresholded t-tests scalpmaps are shown for each condition (black and white maps). Bottom maps show the interaction between the local effect and the current global rule (current block type): it mathematically corresponds to the main effect of the global violation ([LDGD−LSGS] − [LDGS−LSGD] = [LDGD+LSGD] − [LSGS+LDGS]), and shows that the temporal window of the local effect is not affected by the current global rule.

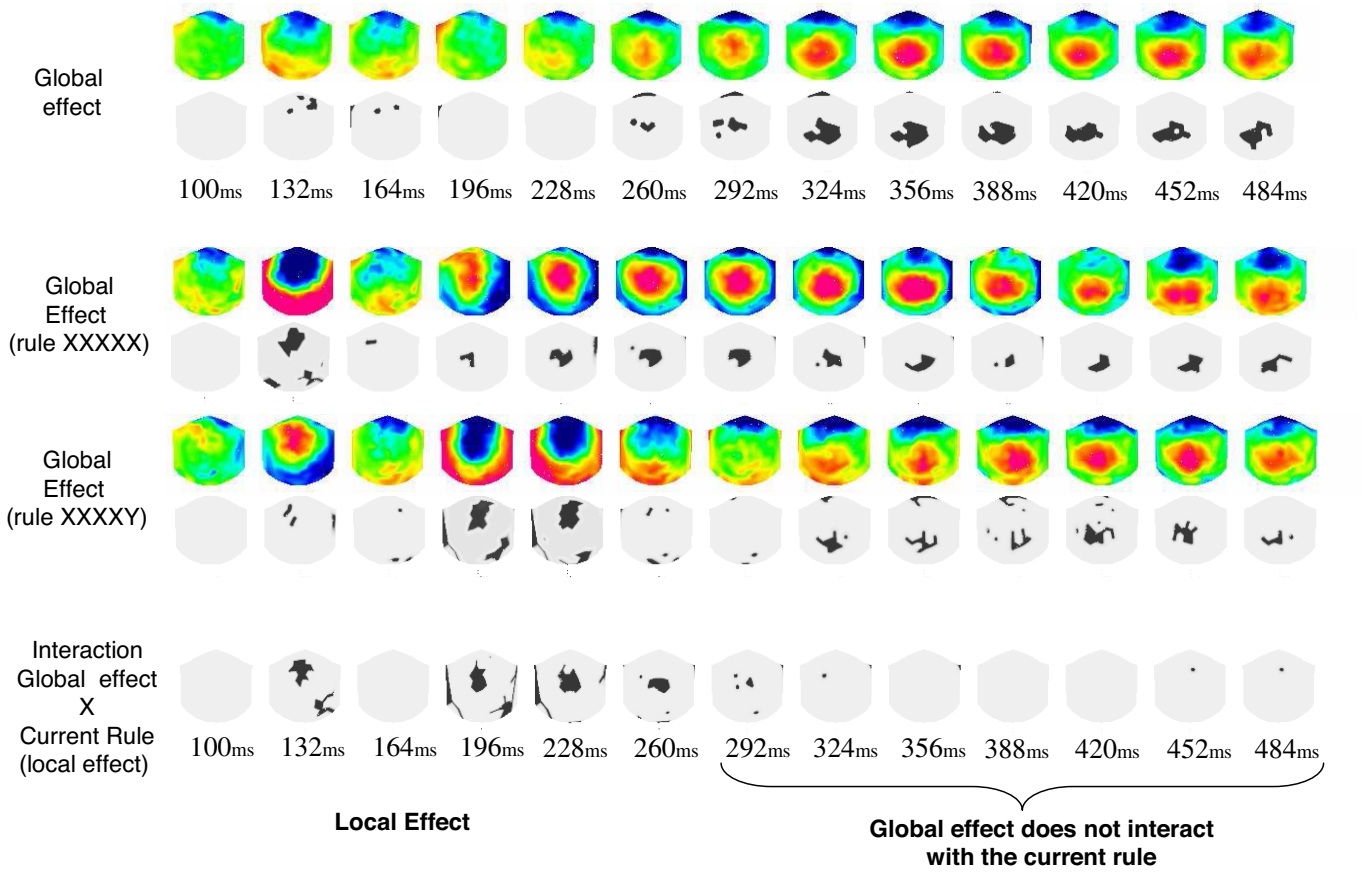

Fig. S2. Global effect split by current global regularity in the counting group. Averaged voltage scalpmaps of the global effect subtractions are plotted separately for the two global rules (LDGD-LSGS and LSGD-LDGS) (top) from 100 to 484 ms after the onset of the fifth sound. Corresponding thresholded *t*-tests scalpmaps are shown for each condition (black and white maps). Bottom maps show the interaction between the global effect and the current global rule (current block type): it mathematically corresponds to the main effect of the local violation ([LDGD−LSGS] − [LSGD−LDGS] = [LDGD+LDGS] − [LSGS+LSGD]), and shows that the temporal window of the global effect is not affected by the current global rule.

Table S1. Summary of fMRI peak of activations for the local and global effects

Effect	Structure	MNI Coordinates	*T* value
Local effect	Right STG	54 −18 3	5.26
Local effect	Left STG	33 −15 5	4.83
Global effect	Right DLPC	54 9 −9	7.69
Global effect	Left DLPFC	−51 9 6	5.95
Global effect	Anterior Cingulate	−9 18 39	6.26
Global effect	Left STG	−54 −27 0	6.64
Global effect	Right STG	57 −18 3	5.49
Global effect	Left Parietal	−12 −66 54	4.61
Global effect	Occipital pole	−6 −102 3	6.77

DLPFC, dorso-lateral prefrontal cortex; STG , superior temporal gyrus. For illustration we show here the coordinates of the highest activation peaks (voxelwise $P < 0.001$, clusterwise > 30 voxels).

Table S2. Synthetic description of DOC patients

Patient	Age	Sexe	Aetiology	Delay (days or months)	Glascow (E/M/V)	CRS-R (total and subscale scores)*
MCS 1	36	Male	Stroke†	24 d	6 (4/1/1)	6 (1 1 0 1 **1** 2)
MCS 2	28	Male	TBI	17 d	5 (3/1/1)	6 (1 **3** 0 1 0 1)
MCS 3	23	Male	Encephalopathy‡	6 m	10 (4/5/1)	17 (**4 5** 2 2 **1** 2)
MCS 4	33	Male	TBI	22 d	9 (3/5/1)	10 (2 **2 4** 1 0 1)
VS 1	67	Male	Anoxia	2 m	7 (4/2/1)	7 (2 1 1 1 0 2)
VS2	62	Male	Encephalopathy§	2 m	4 (2/1/1)	1 (0 0 0 0 0 1)
VS3	31	Male	Anoxia	8 d	4 (2/1/1)	4 (0 0 1 1 0 2)
VS4	61	Male	TBI	30 d	4 (2/1/1)	3 (1 0 0 1 0 1)

The french adaptation (established by Laureys in 2004) of the revised Coma Recovery Scale (36) (CRS-R) was used. TBI, traumatic brain injury.

*For MCS patients, subscale-scores of the CRS-R indicating an MCS status are bolded.

†In addition to his MCS condition, this patient had a typical locked-in syndrome with quadriplegia and aphonia secondary to a ventral pontic stroke. Eye-opening and vertical eye-movements were the only possible voluntary movements. Several weeks later, when this patient recovered a full conscious state, he was still affected by these severe motor deficits.

‡This patient had a congenital deficiency in Pyruvate Deshydrogenase enzyme

§This patient had a MELAS mitochondrial genetic deficiency (Myopathy Encephalopathy Lactate Acidose Stroke)

Other Supporting Information Files

SI Appendix